Chapter 4

The Variogram

4.1 Structural Properties

The positive definite character of the covariance function $C(\boldsymbol{h})$ entails the following properties:

$C(\mathbf{0}) = Var(Z(\boldsymbol{x})) \geq 0$, an *a priori* variance cannot be negative;

$C(\boldsymbol{h}) = C(-\boldsymbol{h})$, the covariance is an even function;

$|C(\boldsymbol{h})| \leq C(\mathbf{0})$, Schwarz's inequality.

Since the degree of correlation between two variables $Z(\boldsymbol{x})$ and $Z(\boldsymbol{x}+\boldsymbol{h})$ generally decreases as the distance $|\boldsymbol{h}|$ between them increases, so, in general, does the covariance function, which decreases from its value at the origin $C(\mathbf{0})$. Correspondingly, the semi-variogram $\gamma(\boldsymbol{h}) = C(\mathbf{0}) - C(\boldsymbol{h})$ increases from its value at the origin, $\gamma(\mathbf{0}) = 0$.

4.1.1 Absence of Correlation

Very often, in practice, the correlation between two variables $Z(\boldsymbol{x})$ and $Z(\boldsymbol{x}+\boldsymbol{h})$ disappears when the distance $|\boldsymbol{h}|$ becomes too large:

$$C(\boldsymbol{h}) \to 0, \quad \text{when} \quad |\boldsymbol{h}| \to \infty,$$

and, in practice, we can put $C(\boldsymbol{h}) = 0$, once $|\boldsymbol{h}| \geq a$. The distance a beyond which $C(\boldsymbol{h})$ can be considered to be equal to zero is called the *range* and it represents the transition from the state in which a spatial correlation exists ($|\boldsymbol{h}| < a$) to the state in which there is absence of correlation ($|\boldsymbol{h}| > a$).

4.1.2 Properties of the Variogram

The definition of the variogram as the variance of increments entails the following properties:

$$\gamma(\mathbf{0}) = 0, \quad \gamma(\boldsymbol{h}) = \gamma(-\boldsymbol{h}) \geq 0.$$

In general, but not always, as $\boldsymbol{h}$ increases, the mean quadratic deviation between the two variables $Z(\boldsymbol{x})$ and $Z(\boldsymbol{x}+\boldsymbol{h})$ tends to increase and so $\gamma(\boldsymbol{h})$ increases from its initial zero value.

Transition Phenomena

Very often, in practice, the semi-variogram stops increasing beyond a certain distance and becomes more or less stable around a limit value $\gamma(\boldsymbol{\infty})$ called a *sill* value, which is simply the *a priori* variance of the random function

$$\gamma(\boldsymbol{\infty}) = Var\{Z(\boldsymbol{x})\} = C(\boldsymbol{0}).$$

In such cases, the *a priori* variance exists as does the covariance. Such variograms, which are characterized by a sill value and a range, are called *transition* models, and correspond to a random function which is not only intrinsic but also second-order stationary.

Zone of Influence

In a transition phenomenon, any data value $z(\boldsymbol{x})$ will be correlated with any other value falling within a radius a of $\boldsymbol{x}$. This correlation and, hence, the influence of one value on the other will decrease as the distance between the two points increases. Thus, the range corresponds to the intuitive idea of a zone of influence of a random function: beyond the distance $|\boldsymbol{h}| = a$, the random variables $Z(\boldsymbol{x})$ and $Z(\boldsymbol{x}+\boldsymbol{h})$ are no longer correlated.

Anisotropies

There is no reason to expect that the mineralization will exhibit the same behavior in every direction, i.e., that the mineralization will be isotropic. In the three-dimensional space, $\boldsymbol{x}$ represents the coordinates (x_u, x_v, x_w) and $\boldsymbol{h}$ represents a vector of modulus $|\boldsymbol{h}|$ and direction $\boldsymbol{\alpha}$. Thus, in condensed form, $\gamma(\boldsymbol{h})$ represents the set of semi-variograms $\gamma(|\boldsymbol{h}|, \boldsymbol{\alpha})$ for each direction $\boldsymbol{\alpha}$.

4.1.3 Nested Structures

Consider two point or quasi-point (very small support) grades $Z(\boldsymbol{x})$ and $Z(\boldsymbol{x}+\boldsymbol{h})$ in a deposit separated by a distance vector $\boldsymbol{h}$. The variability between $Z(\boldsymbol{x})$ and $Z(\boldsymbol{x}+\boldsymbol{h})$, which is characterized by the variogram $E\{[Z(\boldsymbol{x}+\boldsymbol{h}) - Z(\boldsymbol{x})]^2\}$, is due to many causes, which appear over a range of different scales, for example:

(i) at the level of the support ($\boldsymbol{h} = \boldsymbol{0}$), there is a variability due to measurements, i.e., fluctuation in the rate of recovery of the core sample, sampling errors;

(ii) at the petrographic level (e.g., $|\boldsymbol{h}| < 1cm$) a second variability appears due to the transition from one mineralogical element to another;

(iii) at the level of strata or mineralized lenses (e.g., $|\boldsymbol{h}| < 100m$), a third variability may be due to the alternation of strata or of lenses with waste material;

(iv) at the level of a metalliferous province (e.g., $|\boldsymbol{h}| < 100km$), a fourth variability may appear, due to the distribution of the deposits related to the orogenesis of the province; etc.

All these sources or structures of variability, and possibly many more, come into play simultaneously and for all distances $\boldsymbol{h}$. They are called "*nested structures*".

Representation of the Nested Structures

As far as the second-order moments of the random function $Z(\boldsymbol{x})$ are concerned, these nested structures can be conveniently represented as the sum of a number of variograms (or covariances), each one characterizing the variability at a particular scale.

$$\gamma(\boldsymbol{h}) = \gamma_0(\boldsymbol{h}) + \gamma_1(\boldsymbol{h}) + \gamma_2(\boldsymbol{h}) + \ldots + \gamma_k(\boldsymbol{h}).$$

For example, $\gamma_0(\boldsymbol{h})$ may be a transition model (spherical or exponential) which very rapidly reaches its sill value C_0 for distances $\boldsymbol{h}$ that are only slightly larger than the data support. This model thus combines all the micro-variabilities (e.g., measurement errors and petrographic differentiations). $\gamma_1(\boldsymbol{h})$ may be another transition model with a larger range (e.g., $a_1 = 10m$) characterizing the lenticular beds and $\gamma_2(\boldsymbol{h})$ may be a third transition model with a range ($a_2 = 200m$) representing the alternation of strata or the extent of homogeneous mineralized zones.

At smaller distances ($h < 30m$), the observed total variability depends on $\gamma_0(\boldsymbol{h}) + \gamma_1(\boldsymbol{h})$, cf. Figure 4.1, while for large distances it will depend on all the $\gamma_i(\boldsymbol{h})$.

4.1.4 Behavior of the Variogram Near the Origin

The continuity and regularity in space of the random function $Z(\boldsymbol{x})$ and, thus, of the regionalized variable $z(\boldsymbol{x})$ that it represents, are related to the behavior of the variogram near the origin. In order of decreasing regularity, four main types of behavior can be distinguished, see Figure 4.2.

(a) Parabolic Behavior

$\gamma(|\boldsymbol{h}|) \simeq c|\boldsymbol{h}|^2$ when $\boldsymbol{h} \to \boldsymbol{0}$. $\gamma(\boldsymbol{h})$ is differentiable at the origin and the random function is itself differentiable in the mean square sense. This type of behavior is characteristic of a highly regular spatial variability.

(b) Linear Behavior

$\gamma(|\boldsymbol{h}|) \simeq c|\boldsymbol{h}|$ when $\boldsymbol{h} \to \boldsymbol{0}$. $\gamma(\boldsymbol{h})$ is no longer differentiable at the origin but remains continuous at $\boldsymbol{h} = 0$, and, thus, for all $|\boldsymbol{h}|$.

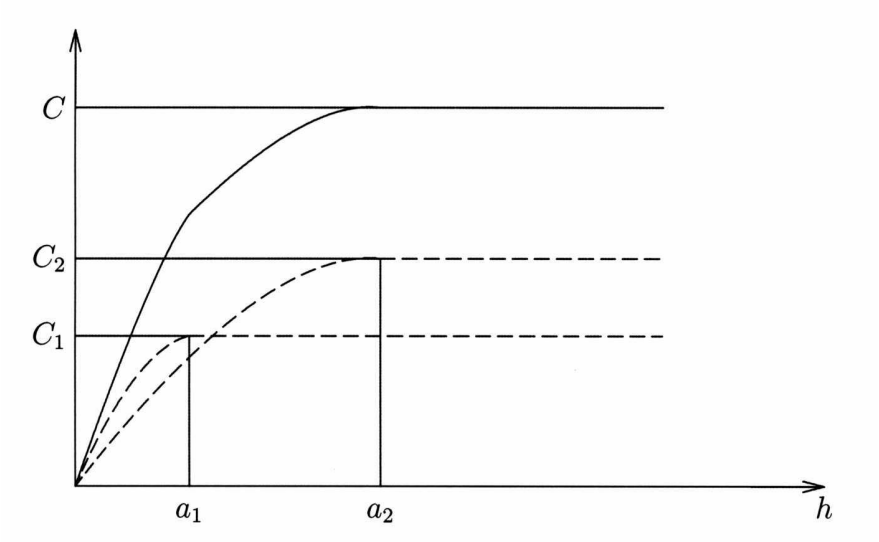

Figure 4.1: Nested Structures.

(c) Discontinuity at the Origin

$\gamma(\boldsymbol{h})$ does not tend towards zero when $\boldsymbol{h}$ tends towards zero, although by definition $\gamma(\mathbf{0}) = 0$. The variability between two values $Z(\boldsymbol{x})$ and $Z(\boldsymbol{x} + \boldsymbol{h})$ taken at two very close points may be quite high and increases as the size of the discontinuity at the origin of $\gamma(\boldsymbol{h})$ increases. This local variability can be compared to the random phenomenon of white noise known to physicists. As the distance $\boldsymbol{h}$ increases, the variability often becomes more continuous and this is reflected in the continuity of $\gamma(\boldsymbol{h})$ for $|\boldsymbol{h}| > 0$.

The discontinuity of the variogram at the origin is called a *nugget effect* and

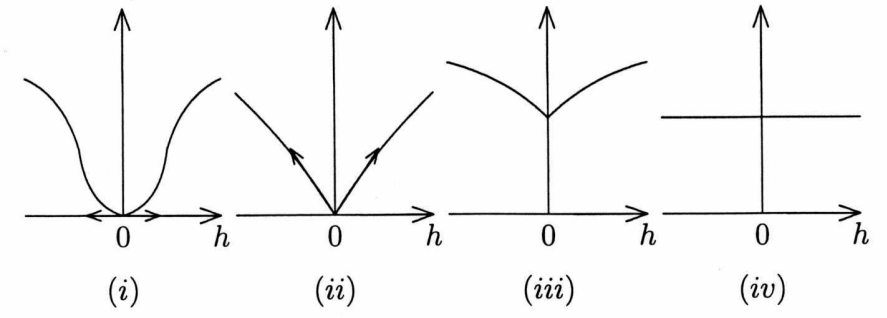

Figure 4.2: Behavior Near the Origin of the Variogram. (i) Parabolic Behavior; (ii) Linear Behavior; (iii) Nugget Effect; (iv) Pure Nugget Effect.

is due both to measurement errors and to micro-variabilities of the mineralization; since the structure of these micro-variabilities is not accessible at the scale at which the data are available, they appear in the form of a white noise.

(d) Pure Nugget Effect

This is the limit case when $\gamma(\boldsymbol{h})$ appears solely as a discontinuity at the origin:

$$\gamma(\mathbf{0}) = 0 \quad \text{and} \quad \gamma(\boldsymbol{h}) = C_0 \quad \text{when} \quad |\boldsymbol{h}| > \epsilon.$$

In practice, such a variogram can be represented as a transition phenomenon with a sill value C_0 and a range $a = \epsilon$, where ϵ is very small in relation to the distances of experimental observation. For all experimental distances, small as they may be, the two random variables $Z(\boldsymbol{x})$ and $Z(\boldsymbol{x} + \boldsymbol{h})$ are uncorrelated. The pure nugget effect thus corresponds to the total absence of auto-correlation. It should be pointed out that such a case is very rare in mining.

4.1.5 Anisotropies

We have already seen that the observed variability of a phenomenon is most often due to many causes ranging over various scales. Consider a nested model $\gamma(\boldsymbol{h})$ consisting of the sum of a micro-structure $\gamma_1(\boldsymbol{h})$ and a macro-structure $\gamma_2(\boldsymbol{h})$:

$$\gamma(\boldsymbol{h}) = \gamma_1(\boldsymbol{h}) + \gamma_2(\boldsymbol{h}) \quad .$$

There is no reason for these two-component structures to have the same directions of anisotropy. Thus, the micro-structure γ_1, characterizing, for example, the measurement errors and the phenomena of diffusion and concretion at very small distances, may be isotropic, while the macro-structure γ_2, characterizing, for example, the lenticular deposits of the mineralization, may reveal directions of preferential alignment of these lenses. In such an example, the structure γ_1 depends only on the modulus $|\boldsymbol{h}|$ of the vector $\boldsymbol{h}$ and it can be represented by any one of the isotropic models presented in Section 4.3. On the other hand, the macro-structure γ_2 will require a model $\gamma_2(|\boldsymbol{h}|, \alpha, \varphi)$ which depends not only on the modulus $|\boldsymbol{h}|$ but also on the direction of the vector $\boldsymbol{h}$.

Anisotropies will be represented by the method of reducing them to the isotropic case either by a linear transformation of the rectangular coordinates $\gamma(h_u, h_v, h_w)$ of the vector $\boldsymbol{h}$ in the case of geometric anisotropy, or by representing separately each of the directional variabilities concerned in the case of zonal anisotropy.

Geometric Anisotropy

A semi-variogram $\gamma(h_u, h_v, h_w)$ or a covariance $C(h_u, h_v, h_w)$ has a geometric anisotropy when the anisotropy can be reduced to isotropy by a mere *linear* transformation

of the coordinates:

$$\gamma(h_u, h_v, h_w) = \gamma'(\sqrt{h_u'^2 + h_v'^2 + h_w'^2})$$

anisotropic isotropic

with

$$h_u' = a_{11}h_u + a_{12}h_v + a_{13}h_w,$$
$$h_v' = a_{21}h_u + a_{22}h_v + a_{23}h_w,$$
$$h_w' = a_{31}h_u + a_{32}h_v + a_{33}h_w,$$

or, in matrix form,

$$\boldsymbol{h}' = A.\boldsymbol{h},$$

where $A = (a_{ij})$ represents the matrix of transformation of the coordinates, and $\boldsymbol{h}$ and $\boldsymbol{h}'$ are column-vectors of the coordinates.

An example is given in Figure 4.4, which shows four semi-variograms for four horizontal directions $\alpha_1, \alpha_2, \alpha_3, \alpha_4$. Spherical models with identical sills and ranges of $a_{\alpha_1}, a_{\alpha_2}, a_{\alpha_3}, a_{\alpha_4}$ have been fitted to these semi-variograms. The directional graph of the ranges, i.e., the variation of the ranges a_{α_i} as a function of the direction α_i, is also shown in Figure 4.3. There are three possible cases.

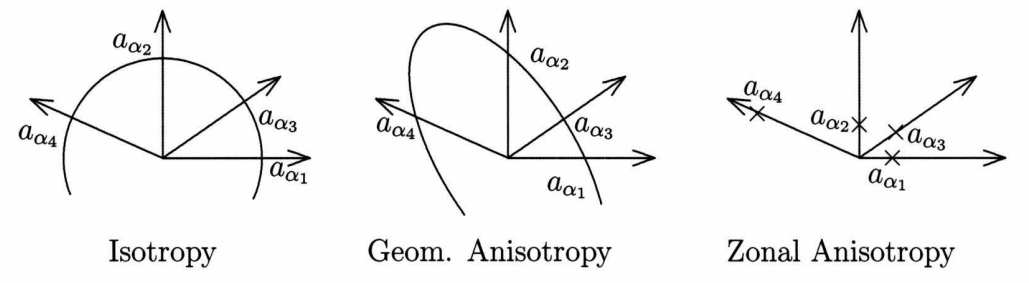

Figure 4.3: Ranges in Case of Anisotropy.

(i) The graph can be approximated to a circle of radius a, i.e., $a_{\alpha_i} \cong a$, for all horizontal directions α_i and the phenomenon can thus be considered as isotropic and characterized by a spherical model of range a.

(ii) The graph can be approximated by an ellipse, i.e., by a shape which is a linear transform of a circle. By applying this linear transformation to the coordinates of vector $\boldsymbol{h}$, the isotropic case is produced (circular graph). The phenomenon is a geometric anisotropy.

(iii) The graph cannot be fitted to a second-degree curve and the second type of anisotropy must be considered, i.e., zonal anisotropy in certain directions, α_4, for example, on Figure 4.3.

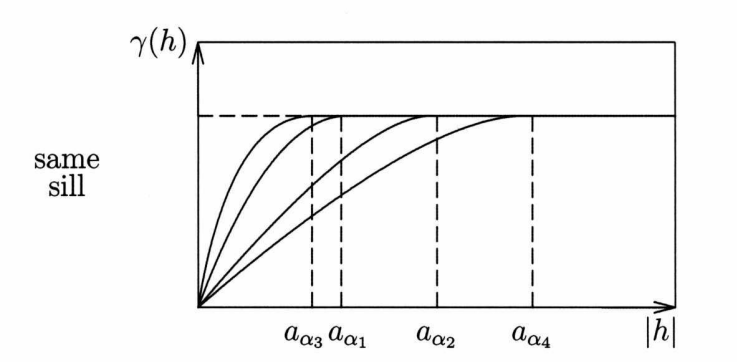

Figure 4.4: Geometric Anisotropy.

Zonal Anisotropy

The model of zonal anisotropy is the one most currently used in practice, since any observed anisotropy which cannot be reduced by a simple linear transformation of coordinates will call for this model.

Let $\gamma(\boldsymbol{h})$ be a nested model characterizing a variability in the three-dimensional space $\gamma(\boldsymbol{h}) = \sum_i \gamma_i(\boldsymbol{h})$, where $\boldsymbol{h}$ is a vector with coordinates (h_u, h_v, h_w). Each of the components $\gamma_i(\boldsymbol{h})$ of this nested model can be anisotropic in $\boldsymbol{h}$, i.e., $\gamma_i(\boldsymbol{h})$ is a function of the three coordinates (h_u, h_v, h_w) rather than of just the modulus $|\boldsymbol{h}|$. Moreover, the anisotropy of $\gamma_i(\boldsymbol{h})$ may be completely different to that of $\gamma_j(\boldsymbol{h})$. Thus, the structure $\gamma_1(\boldsymbol{h})$ may have a geometric anisotropy, while $\gamma_2(\boldsymbol{h})$ is a function of the vertical distance h_w only:

$$\gamma_2(\boldsymbol{h}) = \gamma_2(h_w), \quad \forall h_u, h_v.$$

A third structure may be isotropic in three dimensions: $\gamma_3(\boldsymbol{h}) = \gamma_3(|\boldsymbol{h}|)$.

The model of zonal anisotropy can thus be defined as a nested structure in which each component structure may have its own anisotropy. An obvious anisotropy of the structural function $\gamma(\boldsymbol{h})$ will most often correspond to a genetic anisotropy known beforehand, so that any preferential direction is well known and, thus, can be differentiated when modeling the three-dimensional structural function $\gamma(\boldsymbol{h})$.

4.2 Computation of a Variogram

Let $\boldsymbol{h}$ be a vector of modulus $r = |\boldsymbol{h}|$ and direction $\boldsymbol{\alpha}$ (which may be two-dimensional). If there are n pairs of data separated by the vector $\boldsymbol{h}$, then the experimental semi-variogram in the direction $\boldsymbol{\alpha}$ and for the distance r is expressed as

$$\hat{\gamma}(\boldsymbol{h}) = \hat{\gamma}(r, \boldsymbol{\alpha}) = \frac{1}{2n(\boldsymbol{h})} \sum_{i=1}^{n(\boldsymbol{h})} [z(\boldsymbol{x}_i + \boldsymbol{h}) - z(\boldsymbol{x}_i)]^2 \quad .$$

for a regionalization, and

$$\hat{\gamma}_{kk'}(r, \boldsymbol{\alpha}) = \frac{1}{2n} \sum_{i=1}^{n} [z_k(\boldsymbol{x}_i + \boldsymbol{h}) - z_k(\boldsymbol{x}_i)][z_{k'}(\boldsymbol{x}_i + \boldsymbol{h}) - z_{k'}(\boldsymbol{x}_i)] \quad .$$

for a coregionalization.

Although these expressions are unique and clear, the methods used in constructing variograms depend on the spatial configuration of the available data. Various cases can be distinguished according to whether or not the data are aligned and to whether or not they are regularly spaced along these alignments.

4.2.1 Data Aligned and Regularly Spaced

This category covers most configurations resulting from the systematic reconnaissance of a deposit. The preceding experimental expressions can be applied for each direction $\boldsymbol{\alpha}$ of alignment.

(i) Thus, the configuration represented by a rectilinear drill core in the direction $\boldsymbol{\alpha}$, which has been cut into constant lengths l and analyzed, provides an estimator

$$\hat{\gamma}(kl, \boldsymbol{\alpha}),\ k = 1, 2, \ldots, n/2 \quad ,$$

of the semi-variogram regularized by core samples of length l in the direction $\boldsymbol{\alpha}$ and for distances which are multiple of the basic step size l.

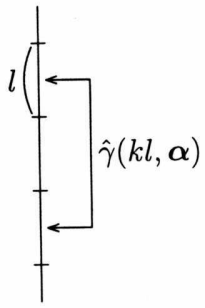

(ii) Vertical channel samples of the same height l and spaced at regular intervals b in the same direction $\boldsymbol{\alpha}$ along a horizontal drift also fall into this category and provide an estimator $\hat{\gamma}(kb, \boldsymbol{\alpha})$. of the semi-variogram, graded over the constant thickness l, in the direction $\boldsymbol{\alpha}$ and for distances which are multiples of the basic step-size b, cf. Figure 4.5.

A simple example of the computation of a variogram in such a situation was already introduced (Section 3.3). The following example should illustrate this in two dimensions.

Example 4.1: (Journel and Huijbregts, 1978(12)) The data set used in this exercise is sufficiently reduced to allow the various directional variograms to be calculated by hand or with the help of a pocket calculator. The example is very simple and is designed to prepare the way for the programming of variogram calculations. If only such a small amount of data were available in practice, the experimental fluctuations on each directional variogram would be so great as to render these variogram curves useless.

The data are located at the corners of a square grid with distance a. The directions to be studied are the two main directions $\boldsymbol{\alpha}_1$ and $\boldsymbol{\alpha}_2$ and the two diagonal

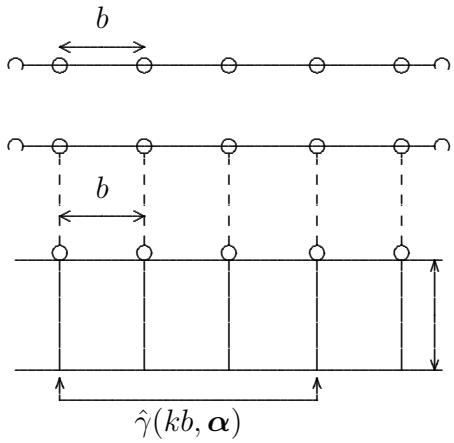

Figure 4.5: Data Aligned and Regularly Spaced (Rectilinear Drill Core).

Table 4.1: Directional Semi-variogram.

Direction	$n(1)$	$\hat{\gamma}(1)$	$n(2)$	$\hat{\gamma}(2)$	$n(3)$	$\hat{\gamma}(3)$
$\boldsymbol{\alpha}_1$	24	4.1	20	8.4	18	12.1
$\boldsymbol{\alpha}_2$	22	4.25	18	8.2	15	10.9
$\boldsymbol{\alpha}_3$	19	5	16	11.9	10	17.3
$\boldsymbol{\alpha}_4$	18	6.5	14	11.3	8	15.4

directions $\boldsymbol{\alpha}_3$ and $\boldsymbol{\alpha}_4$. Note that the basic step size in the diagonal directions is $a\sqrt{2}$, while it is a in the main directions (see Figure 4.6). Table 4.1 gives the number of pairs of data used and the corresponding values of the experimental semi-variogram for each of the four directions and for the first three multiples of the basic step sizes. Isotropy is verified and the mean isotropic semi-variogram is calculated by combining the four directional semi-variograms, cf. Table 4.2 and Figure 4.6. A linear model with no nugget effect can be fitted to the mean semi-variogram:

$$\gamma(|\boldsymbol{h}|) = 4.1|\boldsymbol{h}|/a \quad .$$

Table 4.2: Isotropical, Averaged Semi-variogram.

	$\|\boldsymbol{h}\|$					
	a	$a\sqrt{2}$	2a	$2a\sqrt{2}$	3a	$3a\sqrt{2}$
n	46	37	38	30	33	18
$\hat{\gamma}(\|\boldsymbol{h}\|)$	4.2	5.7	8.3	11.6	11.6	16.3

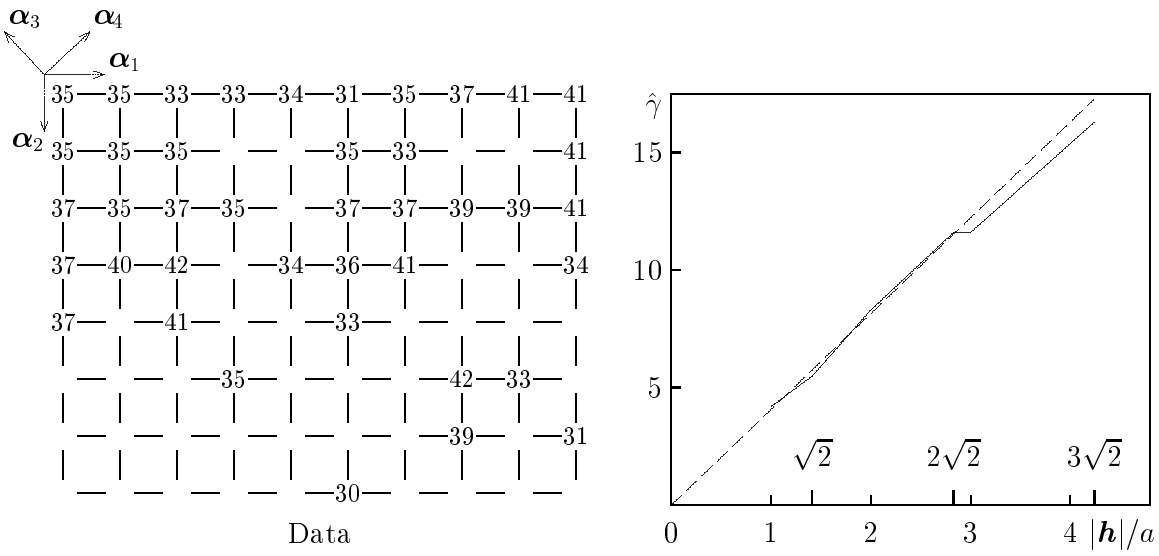

Figure 4.6: Data Arrangement and Semi-variogram.

4.2.2 Aligned but Irregularly Spaced Data

To construct the experimental semi-variogram in the direction of alignment $\boldsymbol{\alpha}$, the data are grouped into distance classes. Every data pair which is separated by a distance $[r \pm \varepsilon(r)]$ is used to estimate the value $\gamma(r)$.

In practice, it is easier to consider a constant tolerance $\varepsilon(r)$ whatever the distance r, i.e., $\varepsilon(r) = \text{constant}$, $\forall r$. Otherwise, $\varepsilon(r)$ should be smaller for smaller distances and larger for greater distances.

This grouping of data pairs into distance classes causes a *smoothing* of the experimental semi-variogram $\hat{\gamma}(r)$ relative to the underlying theoretical semi-variogram $\gamma(r)$, cf. Figure 4.7. If the n available data pairs separated by a distance $r_i \in [r \pm \varepsilon(r)]$ are used instead of those separated by the strict distance r, then it is not $\gamma(r)$ that is being estimated but rather a linear combination of the $\gamma(r_i)$; more precisely, the theoretical mean value

$$\frac{1}{n}\sum_{i=1}^{n} \gamma(r_i, \alpha) \quad .$$

The significance of the effect of this smoothing over the interval $[r \pm \varepsilon(r)]$ decreases as the tolerance $\varepsilon(r)$ becomes smaller with respect to the range of the theoretical model $\gamma(r)$ to be estimated.

In practice, the following points should be heeded.

(i) Take the pseudo-periodicities of the data locations into account when defining the tolerances $\varepsilon(r)$ of the classes.

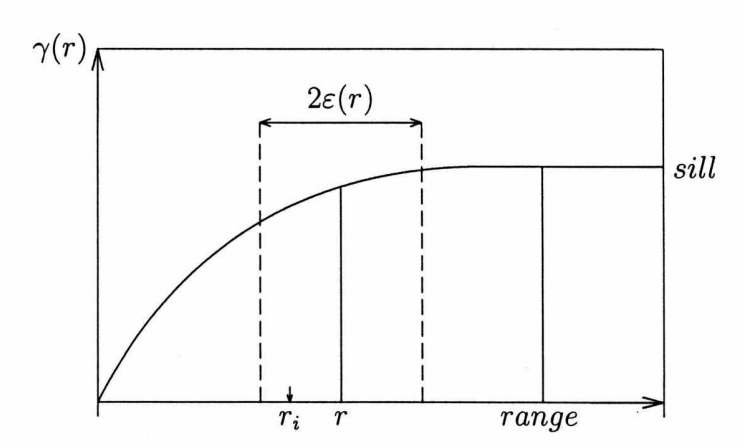

Figure 4.7: Smoothing Effect when Estimating a Variogram.

(ii) Ensure that the section of interest of the variogram (e.g., the increase to the sill value) has been calculated using at least three or four classes; thus, the tolerance $\varepsilon(r)$ should not be too large.

(iii) Ensure that each distance class $[r \pm \varepsilon(r)]$ contains enough pairs so that the corresponding estimator of the variogram is reliable; thus, the tolerance $\varepsilon(r)$ should not be too small.

(iv) Detect any risk of bias due to preferential location of data.

4.2.3 Non-aligned Data

This category can be reduced to one of the former two.

(a) By defining approximately rectilinear pathways passing through the available data locations. Each of these approximate alignments is then treated separately with a possible grouping into distance classes, cf. Figure 4.8. The disadvantage of this method is that all the available data are not used, and it is difficult to program.

(b) By grouping the data into angle classes followed by distance classes, cf. Figure 4.9. To construct the variogram in the direction $\boldsymbol{\alpha}$, each data value $z(\boldsymbol{x}_0)$ is associated with every other value located within the arc defined by $[\boldsymbol{\alpha} \pm \delta(\boldsymbol{\alpha})]$. Within this angle class, the data can be grouped into distance classes $[r \pm \varepsilon(r)]$. The effect of *smoothing*, of course, is again larger.

In the two-dimensional case, the first step will be: Compute the variogram in 4 directions, namely $\alpha \pm \pi/8$.

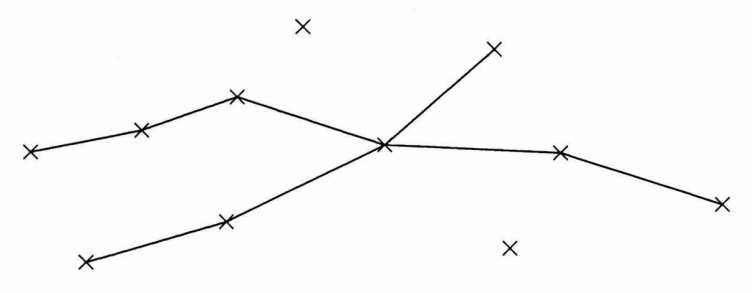

Figure 4.8: Computation of the Variogram: Possible Paths.

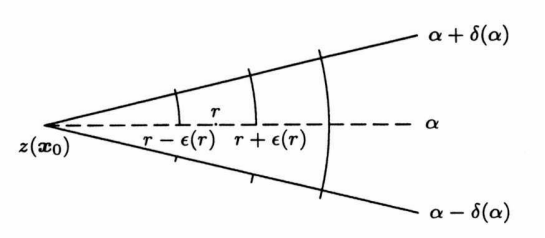

Figure 4.9: Computation of Variograms: Grouping into Angle Classes.

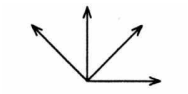

In case different variograms in different directions are indicated, one should decrease the number of classes. (*Anisotropy*: This can often be solved by some corresponding transformation.) Alternatively, one could try to obtain better variograms by grouping: Suppose we have computed K variograms $\hat{\gamma}_k$ $(k = 1, \ldots, K)$ with corresponding n_k pairs of data values. Then a mean variogram with all pairs is simply found by

$$\hat{\gamma}(r) = \frac{1}{\sum_k n_k} \sum_{k=1}^{K} n_k \hat{\gamma}_k(r) \quad .$$

4.3 Variogram Models and Their Fitting

The four main operations of linear geostatistics (variances of estimation and dispersion, regularization and kriging) involve only the structural function of the random function (covariance or variogram). Thus, every geostatistical study begins with the construction of a model designed to characterize the spatial structure of the regionalized variable studied.